

Ionizable drug self-associations and the solubility dependence on pH. Detection of aggregates in saturated solutions using mass spectrometry (ESI-Q-TOF-MS/MS)

Elisabet Fuguet ^{a,b,*}, Xavier Subirats ^a, Clara Ràfols ^a, Elisabeth Bosch ^a, Alex Avdeef ^c

^a Departament d'Enginyeria Química i Química Analítica and Institut de Biomedicina (IBUB), Universitat de Barcelona, Martí i Franquès 1-11, E-08028 Barcelona, Spain

^b Serra-Húnter Program, Generalitat de Catalunya, Barcelona, Spain

^c in-ADME Research, 1732 First Avenue #102, New York, NY 10128, USA

Corresponding author:

Elisabet Fuguet

Martí I Franquès 1-11

08028 Barcelona, Spain

Telf: +34 934039119

Fax: +34 934021233

e-mail: elifuguetj@ub.edu

ABSTRACT

It is widely accepted that solubility-pH profiles of ionizable compounds follow the Henderson-Hasselbalch equation. However, several studies point out that compounds often undergo additional processes in saturated solutions, such as sub-micellar oligomerization, micellar aggregation, or drug-buffer complexation among others, which make the experimental profiles deviate from the behavior predicted by Henderson-Hasselbalch equation. Often, the presence of additional processes is supported by the analysis of experimental data through solubility computer programs. However, the purpose of this work is to experimentally prove the aggregation phenomena for a series of bases for which deviations to the theoretical profile have been observed. To this end, five monoprotic bases (lidocaine, maprotiline, cyproheptadine, bupivacaine, and mifepristone) susceptible to form ionic aggregates in solution have been selected, and mass spectrometry has been the technique of choice to prove the presence of aggregation. High declustering potentials have been applied to prevent aggregates from forming in the ionization source of the mass spectrometer. In addition, haloperidol has been used as negative control, since according to its profile it is not suspected to form ionic aggregates. In all instances, except for haloperidol, the analysis of the saturated solutions revealed the presence of mixed charged dimers (aggregates formed by a neutral molecule and a charged one) and even trimers in case of mifepristone and bupivacaine. For lidocaine, the most soluble of the compounds, the presence of neutral aggregates was also detected. These experiments support the hypothesis that the simple Henderson-Hasselbalch equation may explain the solubility-pH behavior of certain compounds, but it can be somewhat inaccurate in describing the behavior of many other substances.

Keywords: Solubility-pH; shake-flask method; Henderson-Hasselbalch relationships; sub-micellar aggregates; drug-buffer complexes; mass spectrometry

Supporting Information: Table SI-1: Solubility data for maprotiline; Table SI-2: Solubility data for bupivacaine; Table SI-3: Solubility data for lidocaine; Table SI-4: Solubility data for mifepristone; Table SI-5: Solubility data for cyproheptadine; Table SI-6: Solubility data for haloperidol; Figure SI-1: PDXR spectra of the solid phase obtained after phase separation in the shake-flask method for the studied compounds.

1. Introduction

It is generally accepted that for simple molecules, the Henderson-Hasselbalch (HH) equation can predict the pH dependence of thermodynamic solubility. That is, the total solubility of an ionizable molecule at a given pH can be calculated from the ionization constant, pK_a , and the intrinsic (uncharged-form) solubility, S_0 (e.g., $S = S_0 [1 + 10^{+pK_a - pH}]$ for a monoprotic base). In fact, this relationship is frequently used in drug discovery as an easy way to convert the intrinsic solubility value into the equilibrium solubility at physiologically relevant pH values. However, to obtain reliable results it is critical to use precise and carefully determined pK_a and S_0 values.¹ Avdeef *et al.*² critically examined many factors that affect data accuracy and presented concrete recommendations for improving the quality of solubility measurements. Moreover, special attention must be directed to the possibility that the HH equation itself can be substantially inaccurate in describing the observed solubility-pH behavior of certain compounds, most obviously, surface-active molecules.³ Distorted log S -pH profiles are not confined to practically-insoluble molecules. Even soluble drugs, such as the antibiotic cefadroxyl⁴, and amino acids as simple as glycine⁵⁻⁷ do not exhibit the ideal HH-shape in log S -pH profiles.

During solubility measurement, oligomerization (dimers, trimers, ...), aggregation, drug-buffer complexation, drug-coformer complexation (in cocrystal systems), amorphous solids, salts subject to liquid-liquid phase separation (LLPS), and transient oil phases can form, persisting even after 24 h in stirred suspensions. These complications distort the log S -pH profiles from those predicted by the HH equation.⁸

Since aggregation/complexation reactions can strongly depend on temperature, pH, and concentration of reactants added to the saturated solutions, the interpretation of solubility measurements, particularly when the molecules are ionizable, can be challenging.

There are several classical studies of aggregation/complexation, drawing on numerous methods to characterize the saturated solutions. The solubility-pH profiles of phenobarbital, barbital, and oxytetracycline⁹ showed anomalous shapes, which could not be accurately described by the HH equations. In the case of saturated micellar solutions of prostaglandin $F_{2\alpha}$, Roseman and Yalkowsky¹⁰ appeared to recognize that they could not have used the Krebs-Speakman S_{pH-pK_a} method¹¹ for determining the true aqueous pK_a , due to the obvious distortions in the log S -pH profile. Attwood and Gibson¹² studied the solution properties of tricyclic antidepressant molecules (e.g., nortriptyline, imipramine, and desipramine), using light scattering, conductivity, and pH methods. Micellar aggregation was evident, with 23-51 mM critical micelle concentrations (CMC). Doxycycline forms dimers in the pH 0-6 region.¹³ Stable decamers were postulated for MDL201346A by Streng *et al.*¹⁴ Such aggregates were found to have unusually high and/or very temperature-sensitive solubility. Zhu and Streng,¹⁵ using calorimetry, conductivity, and osmometry measurements, concluded that the self-association of dolasetron to form cationic dimers and trimers was enthalpy driven (by H-bond and/or aromatic ring interactions, but not hydrophobic/electrostatic interactions). Many nonsteroidal antiinflammatory drugs, such as indomethacin, diclofenac, ibuprofen, ketoprofen, naproxen, and sulindac, can self-associate by forming mixed-charge aggregates or micelle-like

structures, with 25-160 mM CMC values.¹⁶ Jinno *et al.*¹⁷ considered the effect of sodium lauryl sulfate (SLS) on the solubility-pH profile of piroxicam. Further analysis of their data indicated the presence of uncharged dimers in the absence of SLS.¹⁸ Bergström *et al.*¹⁹ reported the log S-pH profiles of 25 basic drugs, measured in 0.15 M phosphate buffer media over a 24 h equilibration period. Nineteen of the 25 compounds showed distorted log S-pH profiles, attributable to the formation of drug oligomers/complexes in solution.

A recent series of investigations critically examined cases of such distortions.^{3-4,20-23} A database of intrinsic solubility, S_0 , values with 7122 entries of mostly druglike substances has been assembled, where solubility-pH measurements have been accounted for ionization and temperature effects using a new computational approach.^{24,25} The log S-pH profiles for most of these compounds have been binned according to a shape-distortion classification scheme.⁸ Table 1 shows examples of molecules from seven such classes (some molecules belong to two classes). In the uncharged (1a: $(HA)_2$, 1b: B_2 , 1ab: $(H_2X)_2$) and mix-charged (3a: A^-HA , 3b: HB^+B) classes of aggregates, the molecules are typically poorly soluble, with mean $S_0 \approx 10 \mu\text{M}$. In contrast, the fully-charged aggregate classes (2a: $(A^-)_2$, 2b: $(HB^+)_2$) appear to be represented by more soluble molecules, with mean $S_0 \approx 2.5 \text{ mM}$, although the range of solubility values is extensive.

The interpretation of shape distortion due to aggregation in solution has been corroborated by MS/MS measurements for cefadroxyl in our earlier work.⁴ The shape of the log S-pH cefadroxyl curve suggested the predominance of anionic dimers and trimers in solution above pH 6. The analysis of the solutions between pH 6 and 7 using low ionization energy ESI-Q-TOF-MS/MS indicated direct evidence for the presence of monomers, dimers, and trimers in saturated solution.

Whereas the cefadroxyl analysis focused on just one compound, in the present work we performed a more systematic study using six basic substances. Five of the compounds selected had known tendencies to form ionic aggregates in saturated solutions. An additional compound was selected as negative control, to ensure that the MS method was not creating aggregates during measurement.

Table 1: Types of aggregates ^a

Class 1a (neutral acids, (HA) ₂)	Class 1b (neutral bases, B ₂)		Class 1ab (neutral ampholytes, (H ₂ X) ₂)	Class 2a (anionic acids, (A ⁻) ₂)	Class 2b (cationic bases, (HB ⁺) ₂)		Class 3a (half-charged Anionic, (A ⁻ HA))	Class 3b (half- charged Cationic, (HB ⁺ B))
Benzthiazide Diclofenac Flufenamic Acid Furosemide Glibenclamide Glimepiride Ibuprofen Indomethacin Ketoprofen Naproxen	Acetylpromazine Ametryne Atratone Bupivacaine Butacaine Celiprolol Chlorpromazine Desipramine Desmethyldoxepin Disopyramide Doxepin Fendiline Haloperidol Ipatone Ketoconazole	Lidocaine Miconazole Nortriptyline Papaverine Pindolol Procyclidine Prometone Simatone Simetryne Terazosin Terfenadine Thioridazine Thiabendazole Trietatone Trifluoperazine	Hydroxyatrazine Hydroxyipazine Hydroxypropazine Hydroxysimazine Hydroxytrietazine Meloxicam N-Glycylcarbamazepine Niflumic Acid Piroxicam	Ampicillin Cefadroxil Cyclacillin Glycine Diglycine Triglycine Mefenamic Acid Phenylalanine Prostaglandin F _{2α} Theophylline Tixanox Valine Zileuton	Acebutolol Amiodarone Ampicillin Astemizole Isoleucine Lidocaine Orphenadrine Oxytetracycline Papaverine Phenazopyridine Phenylalanine Quinolinol Serine Thiabendazole Trifluoperazine Trihexyphenodryl Valine Verapamil	Pentaglycine Hexaglycine Hydralazine Isoleucine Lidocaine Orphenadrine Oxytetracycline Papaverine Phenazopyridine Phenylalanine Quinolinol Serine Thiabendazole Trifluoperazine Trihexyphenodryl Valine Verapamil	Glibenclamide Indomethacin Niclosamide Tixanox	Dipyridamole Fluphenazine Maprotiline Mifepristone Miconazole Pramoxine Promethazine Propafenone Propranolol Thiabendazole
log S ₀ ± SD ^b								
-5.2 ± 1.0	-4.9 ± 1.1		-4.8 ± 0.8	-2.5 ± 2.7	-2.7 ± 2.2		-5.7 ± 1.4	-5.3 ± 1.2

^a Classification scheme proposed in reference 13. Class examples selected from the intrinsic solubility database described in reference 28.

^b S₀ values in mol L⁻¹.

2. Materials and methods

2.1. Reagents and materials

Bupivacaine hydrochloride (99%), haloperidol (>98%), lidocaine (>98%), maprotiline hydrochloride (>99%), mifepristone (>98%), and cyproheptadine hydrochloride (99%) were obtained from Sigma-Aldrich (St. Louis, MO, USA).

The following chemicals were used to prepare buffer solutions: acetic acid (>99%), formic acid (98%), and ethylenediamine (>98.8) from J. T. Baker (Center Valley, PA, USA), ammonia solution (25%) and trifluoroacetic acid (>99%) from Merck (Darmstadt, Germany), and ammonium bicarbonate (>99%) from Fluka (Buchs, Switzerland). To reach the desired pH value, 1 M sodium hydroxide or hydrochloric acid were added. The ionic strength of all buffer solutions was fixed to 0.1 M.

These reagents were used for pK_a determination: dimethyl sulfoxide >99.9% (DMSO), potassium dihydrogen phosphate (>99.5%), 0.5 M potassium hydroxide Titrisol[®] and 0.5 M hydrochloric acid Titrisol[®] from Merck. Potassium chloride >99% was from Sigma.

For HPLC quantification, formic acid, sodium formate (>99%, Fluka), and methanol (HPLC gradient grade) from Fisher Scientific (Loughborough, UK) were used.

Water was purified by a Milli-Q plus system from Millipore (Bedford, MA, USA), with a resistivity of 18.2 M Ω cm.

2.2. Instrumentation

All pH measurements were taken with a Ross combination electrode Orion 8102 from Thermo Fisher Scientific (Waltham, MA, USA) in a Crison micro-pH 2002 potentiometer with a precision of ± 0.1 mV (± 0.002 pH units) from Crison Instruments S.A. (Alella, Spain).

In the shake-flask solubility determination, a Movil-RoD from Selecta (Abrera, Spain) rotational stirrer was used to mix the samples. Centrifugation was done in a Rotanta 460RS centrifuge from Hettich Lab Technology (Tuttlingen, Germany), at 3500 rpm for 30 minutes at controlled temperature (25 °C). The concentration in the supernatant was quantified by liquid chromatography, using a Shimadzu (Kyoto, Japan) liquid chromatograph, equipped with two Shimadzu LC-10AD pumps, and a Shimadzu SPD-10AV detector. Temperature was controlled at 25.0 ± 0.1 °C with a Shimadzu CTO-10AS column oven. The reversed-phase HPLC measurements were carried out on a Symmetry C18 column, with 5 μ m particle size and dimensions of 4.6x150 mm from Waters (Milford, MA, USA).

The apparatus used to perform pK_a determinations was a PCA200 from Sirius Analytical Instruments Ltd. (Forest Row, UK), equipped with a Sirius D-PAS spectrometer, a bifurcated fiber-optic dip probe from Hellma Analytics (Müllheim, Germany) with path length of 1 cm, and a two channels solvent degasser from SMI-LabHut Ltd. (Churcham, UK). The apparatus was controlled from a computer running the RefinementPro2 software.

An ESI-Q-TOF-MS/MS instrument (Q-Star) from Applied Biosystems (Foster City, CA, USA) was used for the MS and MS/MS measurements. The instrument was calibrated for exact mass calculation with the Agilent calibration solution in positive mode (mass range 200-1500 Da). Compounds were analyzed in positive mode and the settings were: ion spray voltage 4500 V, ion source gas (N₂) 20 arbitrary units (a.u.), curtain gas (N₂) 35 a.u., declustering potential 200 V, and focusing potential 300 V. For MS/MS experiments the settings were: collision gas (N₂) 5 a.u., and collision energy 35 V. Saturated samples were infused at a rate of 10-15 µL/min. Analyst QS 2.0 software from Applied Biosystems was used for data acquisition and processing.

The powder X-Ray diffraction (PXRD) characterization was performed using a PANalytical X'Pert PRO MPD θ/θ powder diffractometer of 240 mm radius equipped with a PIXcel detector from PANalytical B.V. (Almelo, The Netherlands). The apparatus was set in a configuration of convergent beam with a focalizing mirror and a transmission geometry, with flat samples sandwiched between low absorbing films. The detector active length was 3.347°. Work power was 45 kV – 40 mA with a defined beam height of 0.4 mm. Five repeated scans were done from 2 to 60 2 θ ° with a step size of 0.026 2 θ ° and a measuring time of 40 seconds per step.

2.3 Procedures

2.3.1 Solubility protocol

Solubility measurements were performed following the consensus recommendations described elsewhere.² For each compound, buffers at different pH values were selected to cover the full solubility-pH profile. All buffers were MS compatible. Samples were prepared adding a given amount of solid compound (enough to obtain saturated solutions) to 3 mL of the buffered solution. Then the solutions were stirred at controlled temperature (25.0 ± 0.2 °C) for 24 h. However, after 4 h of agitation, the pH of solution was checked and, if necessary, readjusted to the initial value with small amounts of 1 M hydrochloric acid or 1 M sodium hydroxide solution. After the 24 h stirring, samples were let stand for 24 more hours to reach equilibrium.^{2,26,27} Finally, pH was measured again. Phase separation was done by centrifugation for all compounds except for bupivacaine, which presented an extensive amount of solid in suspension after centrifugation. It was filtered through non-sterile 4 mm Millex-LH membrane 0.45 µm pore size filters, with hydrophobic PTFE membrane from Millipore. Filter surface was preconditioned with a small volume of the saturated solution for 20 min to minimize surface adsorption, and the first 0.5 mL of filtered solution were discarded.

The remaining solid was dried under vacuum for 30 minutes and stored at 4 °C until PXRD analysis. The amount of compound in the supernatants was quantified by liquid chromatography. Mobile phase was composed of a 0.1 M formic acid/sodium formate solution at pH 3.5 and methanol. To obtain reasonable retention times for all compounds different methanol percentages (ranging from 25 to 75%) were used in the mobile phase. Elution was in isocratic mode. Flow rate was 1 mL/min, the injection volume was 10 µL, and the detection wavelengths were set between 214 and 306 nm, depending on the compound. To quantify, five standard solutions were prepared in the linear range for each substance. Standards were dissolved in a methanol/water mixture in the same proportion as the mobile phase used for its

analysis. Linearity of the calibration curve was checked, and the limit of quantification determined. In a first attempt, saturated supernatants were injected directly, and when necessary, they were appropriately diluted in water to make them fit in the range of calibration.

The supernatants of some of the samples (mostly those at pH values located in the diagonal region of the *S*-pH profiles, where aggregate species were suspected to form) were also used to test the presence of aggregates through MS measurements.

2.3.2. pK_a determination procedure

All measurements were performed in the PCA200 instrument, in 0.15 M KCl aqueous solution, under argon atmosphere, at 25.0 ± 0.1 °C, and using standardized 0.5 M HCl and 0.5 M KOH as titrants. The pH electrode (Ag/AgCl, Sirius Analytical Instruments Ltd.) was calibrated titrimetrically in the pH range 1.8-12.2. Temperature was periodically monitored during the measurement.

For potentiometric measurements, a given amount of compound (5 mg) was dissolved in 15 mL of a 0.15 M KCl aqueous solution. The sample was pre-acidified to pH 1.8 with 0.5 M standardized HCl. Then it was titrated with standardized 0.5 M KOH.

In spectrophotometric measurements, a 10 mM stock solution of sample was prepared in DMSO. 50 μ L of sample stock solution and 0.25 mL of a 15 mM potassium dihydrogenphosphate buffer were added to 10 mL of a 0.15 M KCl solution. The pH of the sample solution was adjusted to 1.8 with 0.5 M HCl before starting the titration, and then the titration was done using 0.5 M KOH. The UV absorption spectra of the solution were continuously monitored in the titration vial by a fiber optic dip-probe.

A minimum of three measurements for each compound were carried out, and the pK_a values were calculated through the RefinementPro software (Sirius Analytical Instruments, Ltd.).

2.4 Refinement of intrinsic solubility and aggregation constants

The solubility analysis computer program, *pDISOL-X*TM (in ADME Research), was used in this study.²⁰ Briefly, the method uses solubility as a function of pH as measured input data, along with standard deviations, $SD(\log S)$. The mass action algorithm considers the contribution of all species proposed to be present in solution, including all buffer components. The approach does not assume the validity of the HH relationship, nor does it depend on any explicitly derived extensions of the HH equations. The mass action algorithm derives its own implicit equations internally, given any practical number of reactions and estimated constants, which are subsequently refined by weighted nonlinear least-squares regression. The presence of specific aggregates or buffer-drug species can be tested. Solubility equations for the various cases of aggregation as well as the mass balance equations were published in previous works.²⁸ The program assumes an initial condition of a suspension of the solid drug in a solution, ideally with the suspension saturated over a wide range of pH. The program calculates the distribution of species resulting from additions of standardized strong-acid

titrant HCl to simulate the suspension pH speciation down to $\text{pH} < 1$, the staging point for the subsequent operation. From there, a sequence of perturbations with strong-base titrant (*e.g.*, NaOH) is simulated, and solubility calculated at each point in small pH increments, until $\text{pH} > 12$ is reached. The ionic strength, I , is rigorously calculated at each step, and pK_a values (as well as aggregation and complexation constants) are accordingly adjusted for changes in ionic strength from a benchmark level, here set at 0.1 M.²⁸

At the end of the pH-speciation simulation, the calculated $\log S$ vs. pH curve is compared to measured $\log S$ vs. pH. A user-supervised $\log S$ -weighted nonlinear least squares refinement commences to refine the user-proposed solution model, using internally-derived analytical expressions for the differential equations in the regression procedure. The process is repeated until the differences between calculated and measured $\log S$ values reach a minimum.

3. Results and discussion

The presence of aggregates in solution has been tested for six basic compounds: maprotiline, mifepristone, lidocaine, bupivacaine, cyproheptadine, and haloperidol. The selection of these compounds was done according to the experimental $\log S$ -pH profiles from literature.²¹ The analysis of those profiles reveals that all compounds except for haloperidol (selected in the present work as a negative control), are susceptible to form ionic aggregates in solution (classes 2b and 3b, Table 1). This is supported by the deviations of the experimental profiles compared to HH theoretical profiles. However, deviations in the low-pH region may not only be attributed to self-aggregation, but also to complexation of the ionic species with buffer components, especially when concentrated phosphate buffer is used, which is the case in those profiles.^{8,21} A recent study based on desipramine hydrochloride reveals that the use of phosphate buffer solutions may increase the complexity of basic systems, since phosphate complexes are present in solution and several phosphate solid forms of the basic compound may precipitate.²⁹

In order to test the self-aggregation hypothesis, we determined the profiles of the six mentioned drugs selecting buffers other than phosphate and probed the existence of aggregates by mass spectrometry.

3.1. Use of mass spectrometry to test the presence of aggregates in saturated solutions

Mass spectrometry is a suitable technique to test the aggregation phenomena because it allows the detection of charged compounds/aggregates in solution. The technique offers several advantages, such as high sensitivity and specificity, while using only small amounts of sample. It provides information about the structure and molecular weight of compounds and allows qualitative and quantitative determinations. Moreover, it is a common technique present in many analytical laboratories. Nevertheless, there are some factors that must be controlled when working with ESI-MS. One of these concerns the ease of ionization of each compound. Ionization depends on the properties of the specific compound (chemical structure, proton affinity) and on factors related to the solution medium, such as pH. Low pH

solutions favor positive ionization, whereas ionization is quite unfavorable in high pH solutions. Moreover, aggregates may be created in the ionization source of the mass spectrometer. For this reason, in our case, it is especially important to select a negative control (*i.e.*, a compound which is not expected to form charged aggregates, *e.g.*, haloperidol in our case) to certify that aggregates are not generated systematically in the ionization source. In addition to the use of the negative control, experiments must be performed at remarkably high declustering potentials (+200 V) to ensure that detected aggregates come from the solution itself and are not formed in the ionization source.

Among the saturated solutions used to obtain the log *S*-pH profiles, two were selected to perform a qualitative MS study about the presence of aggregates: a solution at a low pH, where compounds are mainly ionized, and a second solution at pH 11, where compounds are in their neutral form. The solution at high pH was selected to see whether the presence of neutral aggregates could also be detected, although we already knew that this pH would not favor ionization. Figure 1 shows the MS spectra of the six drugs in non-alkaline pH, as well as the spectrum of lidocaine at pH 11.0. Table 2 summarizes the qualitative results obtained through the MS determinations. Table 3 lists the various equilibrium constants and the p*K*_a values of the compounds.

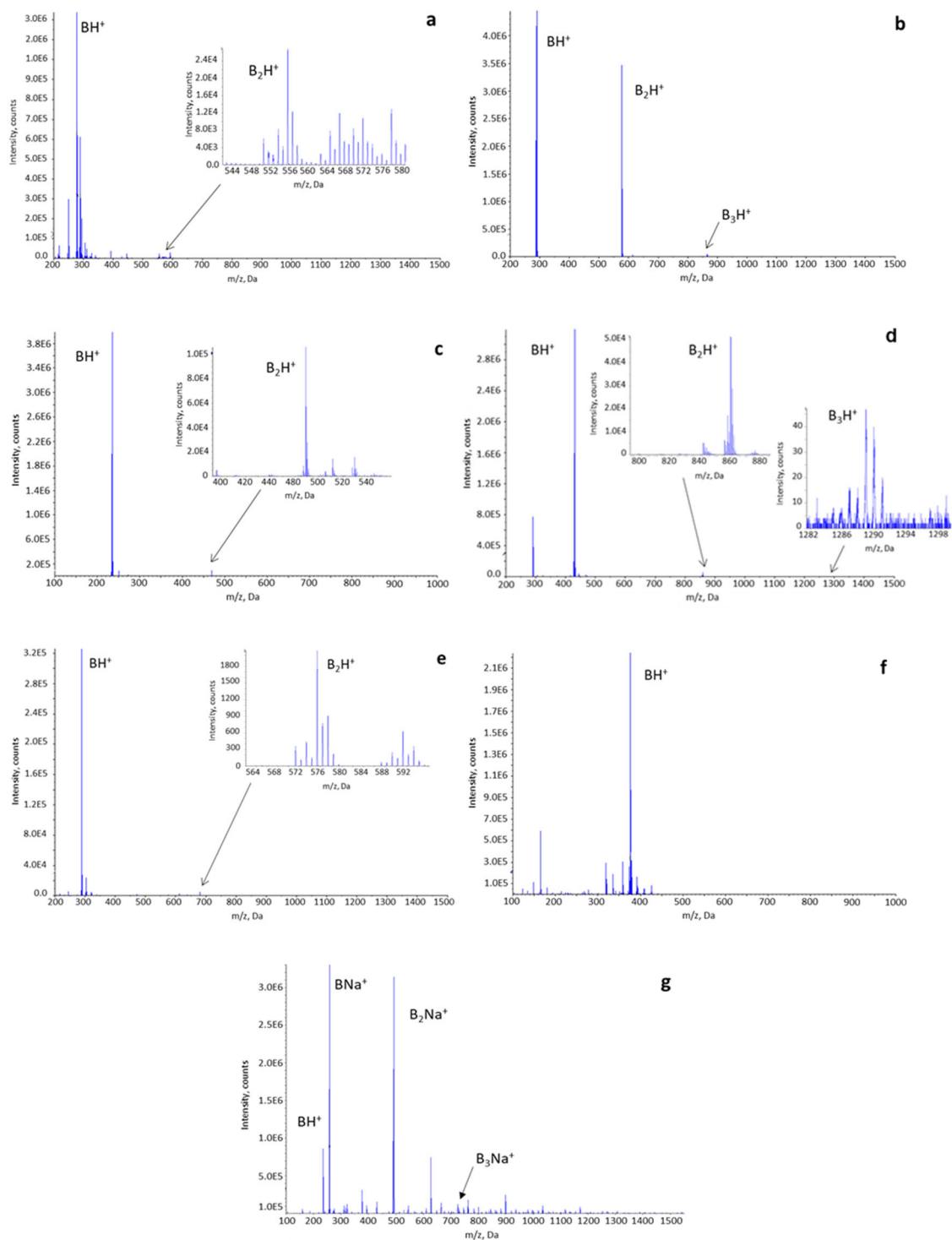


Figure 1: MS spectra of the saturated solutions of the compounds under study. (a) Maprotiline·HCl (pH = 8.9); (b) Bupivacaine·HCl (pH = 5.8); (c) Lidocaine (pH = 7.6); (d) Mifepristone (pH = 3.2); (e) Cyproheptadine·HCl·1.5H₂O (pH = 7.7) ; (f) Haloperidol (pH = 5.7); (g) Lidocaine (pH = 11).

Table 2: Mass spectrometry measurements results

Compound	pH	Aggregates	Observed Species (Mass, Da)
Maprotiline	8.9	Yes	BH ⁺ (278), B ₂ H ⁺ (555)
	11	Not detected	BH ⁺ (278)
Bupivacaine	5.8	Yes	BH ⁺ (289), B ₂ H ⁺ (577), B ₃ H ⁺ (865)
	11	Not detected	BH ⁺ (289)
Lidocaine	7.6	Yes	BH ⁺ (235), B ₂ H ⁺ (469)
	11	Yes	BH ⁺ (235), BNa ⁺ (257), B ₂ Na ⁺ (491), B ₃ Na ⁺ (725)
Mifepristone	3.2	Yes	BH ⁺ (430), B ₂ H ⁺ (859), B ₃ H ⁺ (1288)
	11	Not detected	BH ⁺ (430)
Cyproheptadine	7.7	Yes	BH ⁺ (288), B ₂ H ⁺ (575)
	11	Not detected	BH ⁺ (288)
Haloperidol (negative control)	5.7	Not detected	BH ⁺ (376)
	11	Not detected	BH ⁺ (376)

Table 3: Acidity constants (thermodynamic quantities at 25 °C) of the studied compounds. Logarithm of the intrinsic solubility (in mol L⁻¹), and aggregation constants obtained from the analysis of the measured solubility-pH data (*pDISOL-X* Software).

Compound	pK _a ± SD	log S ₀ ± SD	Aggregation equilibria	log K _{agg} ± SD
Maprotiline	10.20 ± 0.02 ³⁰	-5.06 ± 0.06	B + BH ⁺ ↔ B ₂ H ⁺	5.22 ± 0.11
			BH ⁺ + BH ⁺ ↔ B ₂ H ₂ ²⁺	2.92 ± 0.17
Bupivacaine	8.18 ± 0.09 ³¹	-3.68 ± 0.01	B + BH ⁺ ↔ B ₂ H ⁺	2.60 ± 0.11
			B + B ↔ B ₂	3.01 ± 0.06
Lidocaine	7.97 ± 0.04	-1.98 ± 0.07	B + BH ⁺ ↔ B ₂ H ⁺	1.25 ± 0.20
			B + B ↔ B ₂	1.46 ± 0.16
Mifepristone	5.30 ± 0.04	-5.95 ± 0.09	B + BH ⁺ ↔ B ₂ H ⁺	5.71 ± 0.17
			B + B ↔ B ₂	6.42 ± 0.11
Cyproheptadine	8.92 ± 0.07	-5.40 ± 0.01	B + BH ⁺ ↔ B ₂ H ⁺	4.65 ± 0.28
			B + B ↔ B ₂	5.54 ± 0.13
Haloperidol	8.54 ± 0.09 ³²	-5.86 ± 0.04	B + B ↔ B ₂	5.80 ± 0.15

When solutions at low pH (<pK_a) are analyzed, dimeric mixed aggregates (B + BH⁺ → B₂H⁺) can be detected in all instances, except for haloperidol. In some cases, such as mifepristone and bupivacaine, also trimeric mixed aggregates (B₃H⁺) were observed. The nature of the observed dimers and trimers was confirmed by MS/MS. As an example, Figure 2a shows the MS/MS spectrum of the dimeric species ([B₂H⁺] = 859 Da) of mifepristone, which provides as the main signal the protonated monomer ([BH⁺] = 430 Da). Although only mixed aggregates

have been observed, there is the possibility that cationic dimers or trimers are also present. Mixed aggregates B_2H^+ can be directly observed through MS experiments; however, the mass to charge (m/z) ratio of cationic dimers ($B_2H_2^{2+}$) or trimers ($B_3H_3^{3+}$) has as a result the mass of the protonated monomer, which is the main form observed in all cases. So that, in case cationic dimers or trimers are present, they cannot be distinguished from the monomer signal in the spectra.

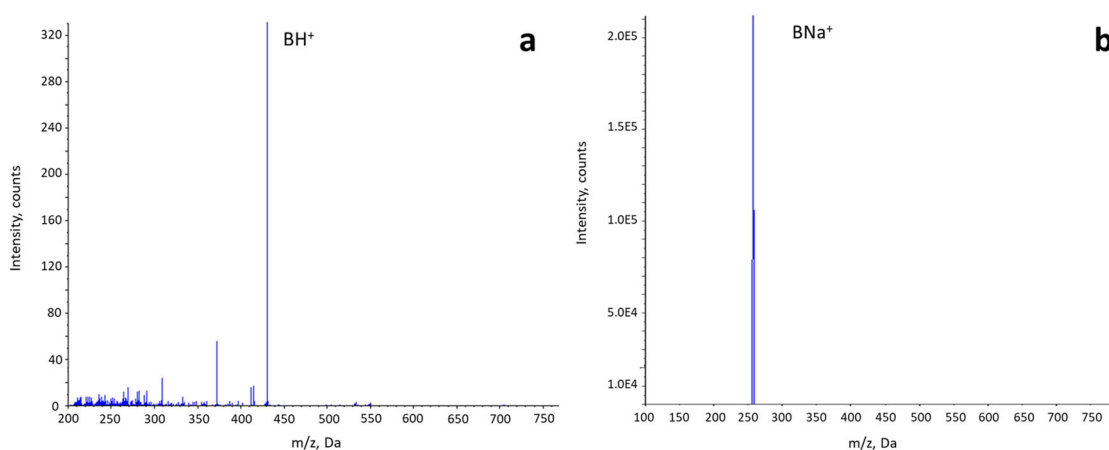


Figure 2: MS/MS spectra of (a) Mifepristone dimer (B_2H^+ : 859 Da); (b) Lidocaine trimer (B_3Na^+ : 725 Da).

When solutions at pH 11 ($>pK_a$) were analyzed, extremely poor signals were obtained. In fact, positive ionization at such high pH values is not good, which makes the detection of neutral aggregates exceedingly difficult. Moreover, at this pH, samples show the lowest concentration since bases have the lowest solubility in highly alkaline solutions. Although the negative ionization mode was also tried, detection was even worse than in positive mode. Lidocaine ($pK_a = 7.97$) is the only compound in which aggregation at pH 11 could be detected. Indeed, it is the most soluble of all studied compounds, and this could be one of the reasons why neutral aggregates were observed only for lidocaine. However, the observed signals correspond mostly to sodium adducts instead of protonated species. As seen in Table 2 and Figure 1g, the spectrum reveals the protonated compound (235 Da), although the signal is low compared to the sodium adduct (257 Da). Neutral dimers (491 Da) and trimers (725 Da) can be also observed as sodium adducts. Figure 2b shows the MS/MS spectrum of the trimeric species of lidocaine, which gives as only product signal the monomer sodium adduct. The MS spectra of the rest of compounds did not show signals that could be attributed to dimers or trimers. However, this does not necessarily exclude the presence of neutral aggregates in solution. It is possible that aggregates were present, but at a concentration under the limit of detection of the technique. Alternative techniques such as fluorescence spectroscopy³³ or proton nuclear magnetic resonance spectroscopy³⁴ could be tried in these instances to confirm aggregation phenomena.

Haloperidol (the negative control) does not present aggregation at low pH values ($<pK_a$), where the ionic form exists. This is confirmed by the spectrum shown in Figure 1f (pH 5.7), where only the peak corresponding to the monomeric form is observed. This fact suggests that aggregates observed for the rest of drugs are formed in solution, and not in the mass spectrometer.

3.2. Analysis of the solubility-pH profiles

The profiles obtained for the studied compounds are shown in Figure 3a-f. Potentiometrically-determined pK_a values have been used for the calculation of the Henderson-Hasselbalch curves (dashed red line), and in the refinement of the equilibrium models using *pDISOL-X*TM (solid black line). Experimental data are provided in the Supporting Information (Tables SI-1 to SI-6). Table 3 lists the aggregation equilibria applied in the analysis of the experimental data, the corresponding constants, as well as the refined S_0 values. These S_0 values were used in the calculation of the HH profile. The curves from the analysis of previously published data²¹ are included for comparison (solid red lines).

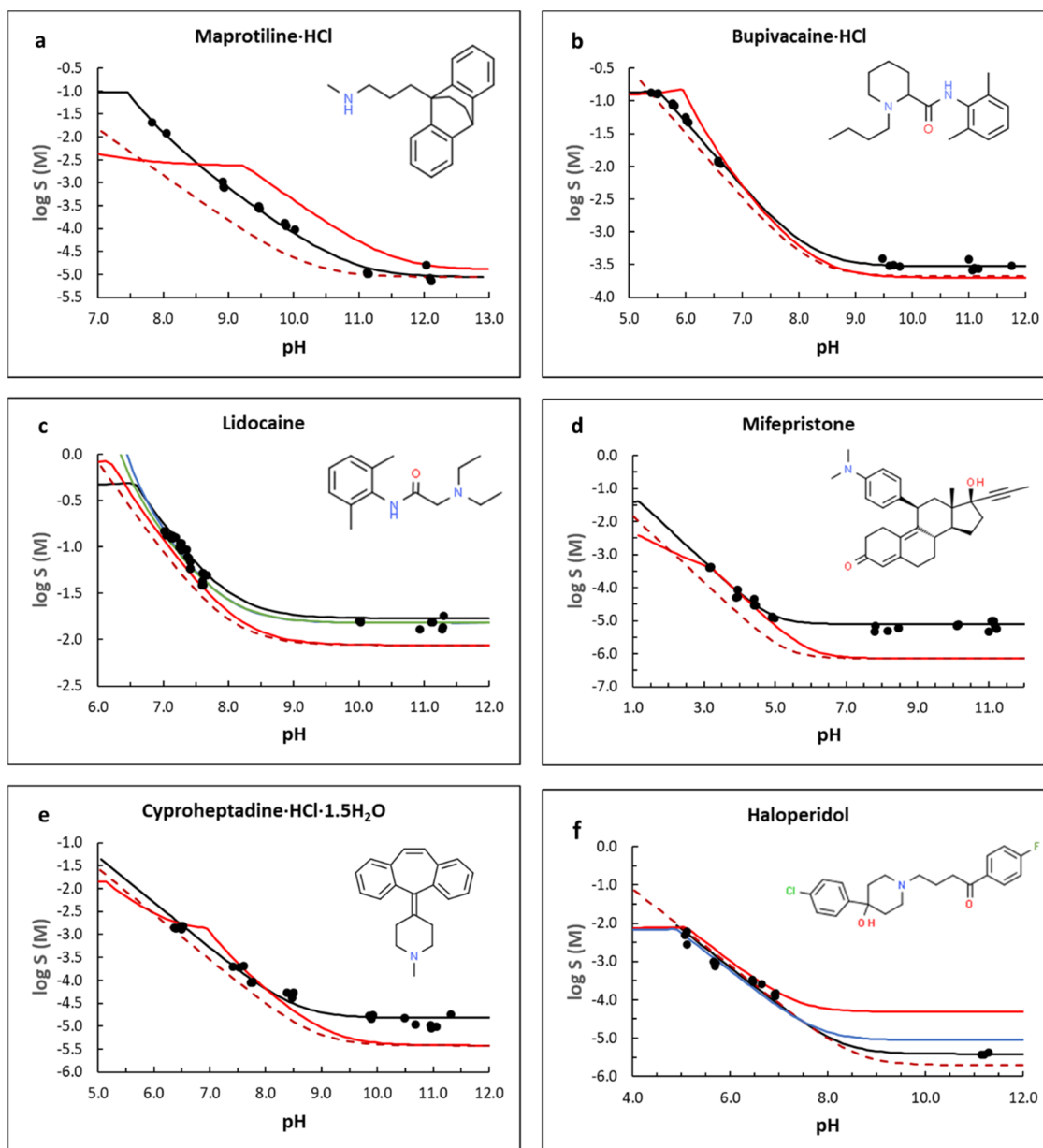


Figure 3: Solubility – pH profiles of the compounds under study. Black circles stand for the experimental points obtained in the present study. Dashed red lines are the Henderson-Hasselbalch profiles. Solid black lines are the best fit obtained in this work. Solid red lines correspond to the fitting of previously published data for the compounds.²¹ Solid green line in lidocaine is the fit of the data from Cassens *et al.*³⁶ Solid blue line in haloperidol is the fit of the data from Li *et al.*³⁷

It is well known that different solid forms of a compound may exhibit different physicochemical properties, as for example solubility. For this reason, the solid state of all experimental points of the profiles have been tested by PXRD analysis (Figure SI-1).

3.2.1. Maprotiline hydrochloride

When solubility experimental points are compared to the theoretical HH curve a clear enhancement of solubility is observed at pH values below the pK_a . Indeed, the best fit suggests self-aggregation between the free base and the protonated species, and also between two molecules of the protonated species (Table 3), which matches with the MS results. It is observed how in the profile from ref. 25 the enhancement of solubility is even more pronounced. In that case different phenomena may contribute to the solubility increase: in a first instance the self-aggregation, and in another instance an additional complexation process between the cationic species with phosphate buffer (mainly with mono- and dihydrogen phosphate anions). Complexation of cationic compounds with phosphate buffer components has also been observed in capillary electrophoresis determinations, where some positively charged bases have shown deviations of electrophoretic mobility when dihydrogen phosphate/monohydrogen phosphate buffer is used.³⁵ Solid state analysis of the remaining solids indicates that the free base precipitates in all instances.

3.2.2. Bupivacaine hydrochloride monohydrate

In this case solubility is also higher than what is expected according to HH equation when pH is below the pK_a . The increase is more pronounced as pH decreases until the hydrochloride salt starts to precipitate. This is confirmed by the solid-state analysis, which indicates that in all instances the free base precipitates, except for the points at the more acidic pH values (below 6), which correspond to the hydrochloride salt. The best fit to the experimental data suggests two types of aggregation: mixed aggregates composed of a neutral and an ionic species (B_2H^+) and neutral aggregates (B_2) (Table 2). MS results at pH 5.8 confirm the presence of dimeric and trimeric mixed aggregates. Compared to the profile shown in the literature,²¹ the enhancement of the solubility is not so pronounced, thus probably phosphate complexation was also playing an important role in the deviations observed in the literature profile.

3.2.3. Lidocaine

Compared to HH profile, the best fit obtained in this work shows a clearly enhanced solubility in the whole pH range. This behavior is remarkably similar to that based on the solubility measurements from by Cassens *et al.*³⁶ (solid green line). The enhanced solubility can be attributed to the presence of neutral and ionic aggregates, as suggested by the fit to the experimental data (Table 2). This is corroborated by MS experiments, which have demonstrated the presence of mixed (at pH values below the pK_a) and neutral aggregates (at pH 11, as sodium adducts) for this compound. Lidocaine free base is the solid form present in all the profile, as indicated by the PXRD characterization.

3.2.4. Mifepristone

Mifepristone behavior is similar to the one of lidocaine. The best fit to the experimental data suggests aggregation between a neutral and an ionized molecule, but also between two neutral molecules (Table 2). The latter aggregates would cause the increase of solubility observed at pH values higher than the pK_a , compared to the HH profile. However, in this case MS could only certify the presence of mixed aggregates due to the poor intensity of the signal at pH 11. PXRD analysis indicates that the same solid form (probably the free base) precipitates along the obtained profile. The profile shown in the literature²¹ presents a similar trend regarding the formation of ionic aggregates, but seems to be free of neutral aggregation as it matches the HH profile in the high pH region.

3.2.5. Cyproheptadine hydrochloride sesquihydrate

The best fit of the experimental data for cyproheptadine also supports the formation of mixed and neutral aggregates. The MS experiments confirm the presence of mixed ionic aggregates at low pH values, but the poor ionization of the compound at pH 11 together with the low solubility value made it impossible to confirm the neutral ones. Contrary to the rest of compounds, the solid state of cyproheptadine is quite complex. Three different solid forms are observed in the pH range studied, according to the PXRD analysis, and none of them matches the commercial form (Figure 4). However, at a given point of the profile (above pH 8.5) the same solid form is always obtained, most likely the free base. None of these solid forms could be identified by comparison to databases or published literature. For this reason, the solubility points at pH values below 8.5 must be considered carefully, since they might follow a different solubility trend than the ones at pH values 8.5 or higher. Similar to mifepristone, the profile shown in the literature²¹ also indicates ionic aggregation but does not show neutral aggregates.

3.2.6. Haloperidol

The profile of haloperidol reveals that only neutral aggregates are formed. In fact, note that all profiles follow the same trend for $pH < 7$, where the ionic form of the compound is the predominant species in solution. This indicates the absence of processes other than that due to solubilization (*i.e.*, absence of additional complexation or aggregation). However, the profiles differ markedly above pH 8. Among the fits, the one of Avdeef²¹ (solid red line) is the one that presents higher distortion compared to HH profile, followed by the one based on the analysis of the data of Li *et al.*³⁷ (solid blue line), and finally the fit obtained in the present work (solid black line). It is well supported that only the uncharged form of haloperidol participates in the HH distortion. It is not entirely clear whether this is a characteristic of a relatively stable “supersaturated” solution, or whether liquid-liquid phase separation (LLPS) phenomenon takes place. In any case, solid state characterization indicates that the same solid form is obtained in the whole profile, which would point to the formation of a stable supersaturated solution.

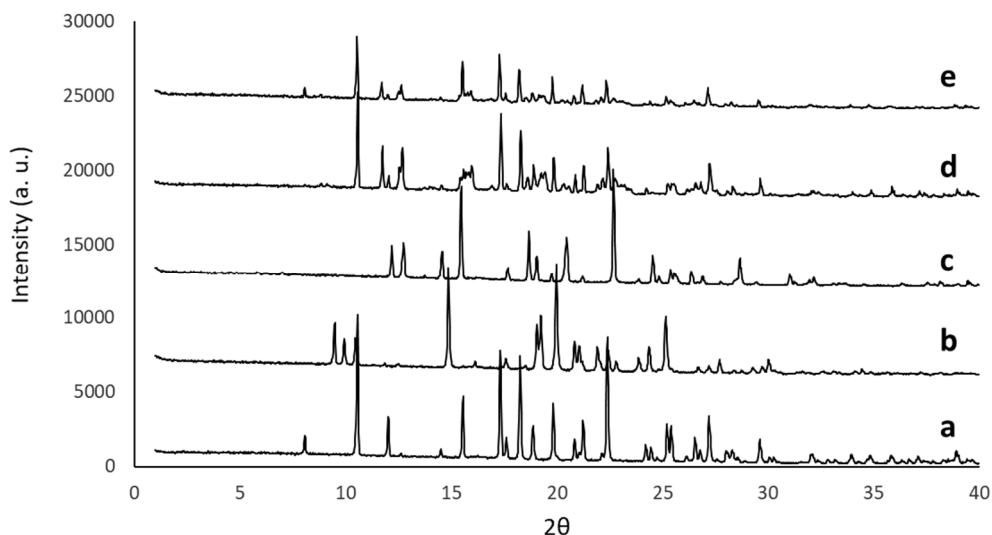


Figure 4: PXRD Characterization of cyproheptadine remaining solid after shake-flask experiments. (a) Commercial form (Cyproheptadine·HCl·1.5H₂O); (b) pH = 6.5; (c) pH = 7; (d) pH = 8.5; (e) pH = 11.

4. Conclusions

The results provided by this study support the evidence that compounds may undergo additional processes other than that due solely to solubilization in saturated solutions. In fact, the work proves the formation of sub-micellar aggregates for all the compounds under study. It is also pointed out that the presence of other processes such as complexation with buffer components is highly probable for some compounds.

MS is a relevant technique to confirm the presence of aggregates, especially ionic ones, although under favorable ionization conditions, neutral aggregates can also be detected. In this work, MS determinations have revealed the presence of mixed charged aggregates (dimers and even trimers) in the saturated solutions of most of the compounds. In the case of lidocaine, the drug with relatively high solubility, the formation of neutral dimers and trimers has also been proved despite the unfavorable ionization conditions.

All in all, this work provides experimental evidence to the idea that when the simple HH equation models overly complicated equilibrium process, it shows slight deviations in the prediction of the solubility-pH behavior of some compounds, especially those surface-active ones. However, further studies are needed to address the long-term stability of the aggregates hypothesized from the evaluation of the shape distortions in log S-pH profiles.

Acknowledgements

The authors from the University of Barcelona are grateful for the financial support of the Spanish government (Project CTQ2017-88179-P AEI/FEDER, UE).

References

- (1) Völgyi, G.; Baka, E.; Box, K. J.; Comer, J. E. A.; Takács-Novák, K. Study of pH-dependent solubility of organic bases. Revisit of Henderson-Hasselbalch relationship. *Anal. Chim. Acta* **2010**, 40-46.
- (2) Avdeef, A.; Fuguet, E.; Llinàs, A.; Ràfols, C.; Bosch, E.; Völgyi, G.; Verbić, T.; Boldyreva, E.; Takács-Novák, K. Equilibrium solubility measurement of ionizable drugs – consensus recommendations for improving data quality. *ADMET & DMPK* **2016**, 4, 117-178.
- (3) Pobudkowska, A.; Ràfols, C.; Subirats, X.; Bosch, E.; Avdeef, A. Phenothiazines solution complexity – determination of pK_a and solubility-pH profiles exhibiting sub-micellar aggregation at 25 and 37 °C. *Eur. J. Pharm. Sci.* **2016**, 93, 163-176.
- (4) Shoghi, E.; Fuguet, E.; Bosch, E.; Rafols, C. Solubility-pH profile of some acidic, basic and amphoteric drugs. *Eur. J. Pharm. Sci.* **2012**, 48, 290–300.
- (5) Needham, T.E., Jr.; Paruta, A.N.; Gerraughty, R.J. Solubility of amino acids in pure solvent systems. *J. Pharm. Sci.* **1971**, 60, 565-567.
- (6) Carta, R.; Tola, G. Solubilities of L-cystine, L-tyrosine, L-leucine, and glycine in aqueous solutions at various pHs and NaCl concentrations. *J. Chem. Eng. Data* **1996**, 41, 414-417.
- (7) Yang, X.; Wang, X.; Ching, C.B. Solubility of form alpha and form gamma of glycine in aqueous solutions. *J. Chem. Eng. Data* **2008**, 53, 1133-1137.
- (8) Avdeef, A. Solubility of sparingly-soluble drugs. *Adv. Drug Deliv. Rev.* **2007**, 59, 568-590.
- (9) Higuchi, T.; Gupta, M.; Busse, L.W. Influence of Electrolytes, pH, and alcohol concentration on the solubilities of acidic drugs. *J. Am. Pharm. Assoc.* **1953**, 42, 157-161.
- (10) Roseman, T.J.; Yalkowsky, S.H. Physical properties of prostaglandin F_{2α}(tromethamine salt): solubility behavior, surface properties, and ionization constants. *J. Pharm. Sci.* **1973**, 62, 1680-1685.
- (11) Krebs, H.A.; Speakman, J.C. Dissociation constant, solubility and the pH value of the solvent. *J. Chem. Soc.* **1945**, 593-595.
- (12) Attwood, D.; Gibson, J. Aggregation of antidepressant drugs in aqueous solution. *J. Pharm. Pharmacol.* **1978**, 30, 176-180.
- (13) Bogardus, J.B.; Blackwood, R.K., Jr. Solubility of doxycycline in aqueous solution. *J. Pharm. Sci.* **1979**, 68, 188-194.
- (14) Streng, W.H.; Yu, D.H.-S.; Zhu, C. Determination of solution aggregation using solubility, conductivity, calorimetry, and pH measurement. *Int. J. Pharm.* **1996**, 135, 43-52.
- (15) Zhu, C.; Streng, W.H. Investigation of drug self-association in aqueous solution using calorimetry, conductivity, and osmometry. *Int. J. Pharm.* **1996**, 130, 159-168.

- (16) Fini, A.; Fazio, G.; Feroci, G. Solubility and solubilization properties of non-steroidal antiinflammatory drugs. *Int. J. Pharm.* **1995**, 126, 95-102.
- (17) Jinno, J.; Oh, D.-M.; Crison, J.R.; Amidon, G.L. Dissolution of ionizable water-insoluble drugs: the combined effect of pH and surfactant, *J. Pharm. Sci.* **2000**, 89, 268-274.
- (18) Avdeef, A.; Voloboy, D.; Foreman, A., Dissolution and solubility. In Testa B.; Van de Waterbeemd H. (Eds.), *Comprehensive Medicinal Chemistry II*: Elsevier, Oxford, UK, 2007.
- (19) Bergström, C.A.S.; Luthman, K.; Artursson, P. Accuracy of calculated pH-dependent aqueous drug solubility. *Eur. J. Pharm. Sci.* **2004**, 22, 387–398.
- (20) Völgyi, G.; Marosi, A.; Takács-Novák, K.; Avdeef, A. Salt solubility products of diprenorphine hydrochloride, codeine and lidocaine hydrochlorides and phosphates – novel method of data analysis not dependent on explicit solubility equations. *ADMET & DMPK* **2013**, 1, 48-62.
- (21) Avdeef, A. Phosphate precipitates and water-soluble aggregates in re-examined solubility-pH data of twenty-five basic drugs. *ADMET & DMPK* **2014**, 2, 43-55.
- (22) Avdeef, A. Anomalous Solubility Behavior of Several Acidic Drugs. *ADMET & DMPK* **2014**, 2, 33-42.
- (23) Butcher, G.; Comer, J.; Avdeef, A. pK_a -critical Interpretations of solubility–pH profiles: PG-300995 and NSC-639829 case studies. *ADMET & DMPK* **2015**, 3, 131-140.
- (24) Avdeef, A. Suggested improvements for measurement of equilibrium solubility-pH of ionizable drugs. *ADMET & DMPK* **2015**, 3, 84-109.
- (25) Avdeef, A. Solubility temperature dependence predicted from 2D structure. *ADMET & DMPK* **2015**, 3, 298-344.
- (26) Baka, E.; Comer, J.E.A.; Takács-Novák, K. Study of equilibrium solubility measurement by saturation shake-flask method using hydrochlorothiazide as model compound. *J. Pharm. Biomed. An.* **2008**, 46, 335-341.
- (27) EPA. *EPA Product Properties Test Guidelines, OPPTS 830.7840, Water Solubility: Column Elution Method; Shake Flask Method. OPPTS 830.7840*, 1998.
- (28) Avdeef, A. *Absorption and Drug Development, Second ed.*: Wiley-Interscience, Hoboken, NJ, 2012.
- (29) Marković, O.S.; Pešić, M.P.; Shah A.V.; Serajuddin, A.T.M.; Verbić, T.Ž.; Avdeef, A. Solubility-pH profile of desipramine hydrochloride in saline phosphate buffer: Enhanced solubility due to drug-buffer aggregates. *Eur. J. Pharm. Sci.* **2019**, 133, 264-274.
- (30) Ruiz, R.; Rosés, M.; Ràfols, C.; Bosch, E. Critical validation of a new simpler approach to estimate aqueous pK_a of drugs sparingly soluble in water. *Anal. Chim. Acta* **2005**, 550, 210–221.

- (31) Fornells, E.; Fuguet, E.; Mañé, M.; Ruiz, R.; Box, K.; Bosch, E.; Ràfols, C. Effect of vinylpyrrolidone polymers on the solubility and supersaturation of drugs; a study using the Cheqsol method. *Eur. J. Pharm. Sci.* **2018**, *117*, 227-235.
- (32) Ràfols, C.; Subirats, X.; Rubio, J.; Rosés, M.; Bosch, E. Lipophilicity of amphoteric and zwitterionic compounds: a comparative study of determination methods. *Talanta* **2017**, *162*, 293-299.
- (33) Tasca, E.; Alba, J.; Galantini, L.; D'Abramo, M.; Giuliani, A. M.; Amadei, A.; Palazzo, G.; Giustini, M. The self-association equilibria of doxorubicin at high concentration and ionic strength characterized by fluorescence spectroscopy and molecular dynamics simulations. *Colloids Surf., A* **2019**, *577*, 517-522.
- (34) Agrawal, P.; Barthwal, S. K.; Barthwal, R. Studies on self-aggregation of anthracycline drugs by restrained molecular dynamics approach using nuclear magnetic resonance spectroscopy supported by absorption, fluorescence, diffusion ordered spectroscopy and mass spectrometry. *Eur. J. Med. Chem.* **2009**, *44*, 1437-1451.
- (35) Fuguet, E.; Reta, M.; Gibert, C.; Rosés, M.; Bosch, E.; Ràfols, C. Critical evaluation of buffering solutions for pK_a determination by capillary electrophoresis. *Electrophoresis* **2008**, *29*, 2841-2851.
- (36) Cassens, J.; Prudic, A.; Ruether, F.; Sadowski, G. Solubility of pharmaceuticals and their salts as a function of pH. *Ind. Eng. Chem. Res.* **2013**, *52*, 2721-2731.
- (37) Li, S.; Doyle, P.; Metz, S.; Royce, A.E.; Serajuddin, A.T.M. Effect of chloride ion on dissolution of different salt forms of haloperidol, a model basic drug. *J. Pharm. Sci.* **2005**, *94*, 2224-2231.

Ionizable drug self-associations and the solubility dependence on pH. Detection of aggregates in saturated solutions using mass spectrometry (ESI-Q-TOF-MS/MS)

Elisabet Fuguet ^{a,b,*}, Xavier Subirats ^a, Clara Ràfols ^a, Elisabeth Bosch ^a, Alex Avdeef ^c

^a Departament d'Enginyeria Química i Química Analítica and Institut de Biomedicina (IBUB), Universitat de Barcelona, Martí i Franquès 1-11, E-08028 Barcelona, Spain

^b Serra-Húnter Program, Generalitat de Catalunya, Barcelona, Spain

^c in-ADME Research, 1732 First Avenue #102, New York, NY 10128, USA

Supporting Information

Table SI-1: Solubility data ($\mu\text{g mL}^{-1}$) for maprotiline

pH	S
7.83	5755.52
8.05	3357.85
8.91	287.98
8.92	226.55
8.94	216.67
9.46	80.28
9.47	83.33
9.48	76.40
9.87	36.89
9.89	31.84
10.02	26.17
12.04	4.48
12.08	2.33
12.10	2.01
11.13	3.12
11.13	2.74
11.15	2.85

Table SI-2: Solubility data ($\mu\text{g mL}^{-1}$) for bupivacaine

pH	S
5.39	38438.00
5.50	36726.32
5.51	37132.97
5.76	26500.50
5.77	24716.99
5.80	24143.47
6.00	16385.07
6.01	14668.04
6.04	13432.98
6.57	3524.90
6.57	3307.12
6.63	3084.48
9.49	113.87
9.60	87.46
9.67	90.12
9.78	85.10
11.00	111.72
11.06	75.28
11.10	78.86
11.10	80.55
11.17	79.98
11.76	88.29

Table SI-3: Solubility data (mg mL⁻¹) for lidocaine

pH	S
7.02	34.57
7.05	31.17
7.13	29.29
7.13	31.00
7.14	28.96
7.15	30.48
7.19	29.91
7.41	13.61
7.41	13.67
7.41	13.90
7.29	21.21
7.25	23.08
7.26	25.73
7.28	21.78
7.28	25.58
7.32	22.48
7.36	18.35
7.36	21.84
7.38	17.84
7.42	16.33
7.59	9.12
7.60	10.01
7.60	12.32
7.61	9.05
7.61	12.15
7.66	11.59
10.01	3.78
10.03	3.72
10.03	3.63
10.93	2.14
10.94	3.03
10.94	2.43
11.11	3.63
11.12	3.59
11.13	3.63
11.28	3.05
11.28	3.19
11.30	4.23

Table SI-4: Solubility data ($\mu\text{g mL}^{-1}$) for mifepristone

pH	S
3.14	169.64
3.16	170.73
3.18	181.00
3.90	21.95
3.93	37.88
3.93	22.62
4.40	19.55
4.41	12.41
4.44	12.69
4.91	5.73
4.92	5.29
5.00	4.82
7.79	1.98
7.82	3.00
8.16	2.10
8.46	2.57
8.47	2.56
10.10	3.09
10.11	2.93
10.15	3.28
11.00	2.03
11.09	4.11
11.14	4.32
11.15	3.72
11.19	2.80
11.22	2.46

Table SI-5: Solubility data ($\mu\text{g mL}^{-1}$) for cyproheptadine

pH	S
6.36	409.99
6.39	390.37
6.48	426.99
6.50	419.06
6.50	377.35
6.52	438.12
7.42	57.48
7.52	55.59
7.60	58.18
7.74	25.15
7.77	25.28
7.78	26.78
8.38	15.28
8.47	12.16
8.50	15.66
9.85	4.79
9.89	4.18
9.91	4.94
10.48	4.33
10.68	3.10
10.96	2.99
10.97	2.59
11.06	2.82
11.31	5.10

Table SI-6: Solubility data ($\mu\text{g mL}^{-1}$) for haloperidol

pH	S
5.07	1428.93
5.11	787.97
5.66	286.12
5.68	217.64
5.70	256.99
6.45	96.39
6.46	83.57
6.64	74.54
6.91	40.94
6.93	35.48
6.95	42.46
11.21	1.06
11.29	1.22

Figure SI-1: PDXR spectra of the solid phase obtained after phase separation in the shake-flask method. Maprotiline free base (A), bupivacaine hydrochloride (B), bupivacaine free base (C), lidocaine free base (D), mifepristone free base (E), and haloperidol free base (F).

